

Two-dimensional transport in disordered carbon and nanocrystalline diamond films

Somnath Bhattacharyya*

School of Physics and DST/NRF Centre of Excellence in Strong Materials, University of the Witwatersrand, Private Bag 3, WITS 2050, Johannesburg, South Africa

(Received 5 November 2007; revised manuscript received 7 May 2008; published 23 June 2008)

We show the contribution of weak localization in two-dimensions as well as electron–electron interactions at low temperature to the delocalized transport in heavily nitrogen-incorporated nanocrystalline diamond (NCD) films via magnetoresistance. The unique carbon-microstructure of the grain-boundary regions, which is significantly different from amorphous conducting carbon films, can exhibit coherent transport in these films over a few tens of nanometers. The large value of the phase decoherence time of electron wave functions together with its weak temperature dependence in NCD films suggest their potential for large area high-speed device applications.

DOI: 10.1103/PhysRevB.77.233407

PACS number(s): 73.50.–h, 73.63.Bd, 73.43.Qt

I. INTRODUCTION

There have been several attempts to understand the outstanding electronic properties of nitrogen-incorporated nanocrystalline diamond (NCD) films recently.^{1–4} At this stage a clear understanding of the unique microstructure of grain boundaries (GB) enhancing the film conductivity will be a prerequisite for practical electronic device applications of this material. As a first approach the conductivity of NCD films prepared with low nitrogen concentration was analyzed using a combination of hopping and activated conduction process [in three-dimensional (3D)] in different temperature regimes.⁴ For heavily doped NCD films yielding high conductivity (e.g., conductivity ≥ 140 S cm⁻¹ and doped with 20% N₂ in gas phase) the activation energy was found to be approaching to zero and the spin density changes dramatically compared to other samples.^{1–3} In this conductivity regime (like metals) the effect of weak localization (WL), quantum interference, and electron–electron (e–e) interactions relative to the classical conductivity can be seen.⁵ Through high negative magnetoresistance (MR), WL of electrons has been shown in nitrogen-doped NCD films.³ We perform a detailed study over a temperature range of about 100 K in heavily doped and highly conducting NCD films¹ and try to determine important parameters, e.g., minimum conductivity (σ_{\min}) and coherence length (L_{ϕ}) not depending particularly on the means of determination of the activation energy (E_a) and magnetic length.³ Recently, we attempted to explain the microstructure of conducting carbon films based on WL through tunnel barriers of *sp*³-bonded carbon.⁶ Evidence for tunnel transport and crossover of dimensionality of WL and e–e interactions, at relatively high temperature, has been observed from temperature-dependent conductivity in two-dimensional (2D) *a*-C films which can be verified from MR study.⁶ Resonant tunneling with a low tunnel effective mass (m^*) in a related system, e.g., artificially grown carbon-superlattice structures, has also been established.⁷ One of our objectives is to implement similar concept in NCD films to explain the transport in GB regions separated by tunnel barriers of nanodiamond crystals. The aim of the work is to the determination of phase coherence time (τ_{ϕ}) from MR to show potential for high-speed applications of these materials.

II. EXPERIMENT

In this report, we mainly focus on the heavily doped NCD films (NCD_{20N}) and also NCD_{10N} films prepared with 20% N₂ and 10% N₂ gas in a plasma reactor, respectively.^{1–4} From the microstructure analysis thin GB (~ 2 nm) of these films has been found free from crystalline or ordered graphitic structures.^{1–5} Conduction through GB of these nanostructured films was compared to conducting *a*-C films, labeled as C₆₀₀, prepared at a substrate temperature of about 600 °C.⁶ Four-probe electrical conductivity and MR data for these films deposited on fused-quartz substrates were measured from 300 K down to 4.2 K and in a field (H) of up to 9 T for NCD films.

III. LOW TEMPERATURE CONDUCTIVITY

First of all, the room temperature conductivity of NCD_{20N} films ($\sigma_{300\text{ K}} \sim 140$ Ω⁻¹ cm⁻¹) is remarkably high compared to 2D C₆₀₀ films ($\sigma_{300\text{ K}} \sim 120$ Ω⁻¹ cm⁻¹) and to NCD_{10N} ($\sigma_{300\text{ K}} \sim 30$ Ω⁻¹ cm⁻¹). For high-conductivity samples $\sigma(T)$ could not be fitted in the intermediate to high-temperature range through a single process, namely, activated or variable range hopping (VRH) conduction, described previously.^{4,6} At lower temperatures, approaching zero Kelvin, a finite value of σ is clearly revealed in all samples [Figs. 1(a) and 1(b) and Fig. 2]. The conductivity of the NCD_{20N} samples shows a $T^{0.5}$ behavior below 20 K [Fig. 1(a)] and $\ln T$ dependence clearly over a wide range, i.e., 20–70 K [Fig. 1(b)], which can be explained by the e–e interactions (in 3D) and WL of electrons (in 2D), respectively.^{8–10} For NCD_{10N} a signature of 2D WL can be seen below 15 K only, i.e., at a much lower temperature than NCD_{20N} films where 2D WL is more pronounced. For C₆₀₀, similar features with a changeover from 3D to 2D (WL) conduction were seen at higher temperature, i.e., 100 K.⁶ Adding these corrections to the Drude conductivity (σ_0) in the disordered metallic regime the total conductivity is expressed as (considering e–e interaction in 3D only)

$$\begin{aligned} \sigma(T) = & \sigma_0 + [\Delta\sigma_L]^{3\text{D}/2\text{D}} + [\Delta\sigma_L]^{3\text{D}} = \sigma_0 + [B \ln T]^{2\text{D}} \\ & + [m T^{1/2}]^{3\text{D}} \text{ or, } = \sigma'_0 + [B' T^{p/2}]^{3\text{D}} + [m' T^{1/2}]^{3\text{D}}. \end{aligned} \quad (1)$$

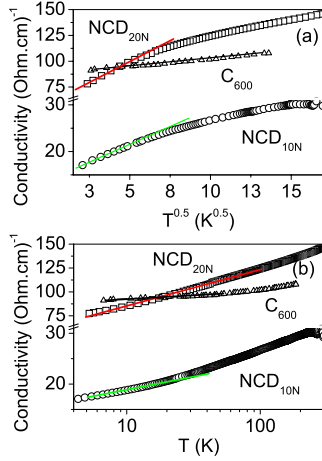


FIG. 1. (Color online) Variation of (a) conductivity versus $T^{0.5}$ (b) conductivity with $\ln(T)$ to show e-e interaction effects in 3D and WL in 2D, respectively.

In general WL correction to $\sigma(T)$ can be expressed as $\Delta\sigma_L^{2D}(T) = e^2/\{\pi h\} \ln(1/L_{Th}) = B \ln(T)$ and $\Delta\sigma_L^{3D}(T) = e^2/\{\pi h L_{Th}\} = e^2/\{\pi h\} T^{p/2}$, where $L_{Th} \equiv$ Thouless length.^{8,9} For WL in 3D theoretical values of ‘ p ’ can be 3/2, 2, or 3 depending on the type of scattering;^{8–10} however they do not produce a proper fit to the present data. A best fit using $\ln T$ and $T^{1/2}$ instead of a $T^{3/2}$ fit for all the samples indicates that both e-e interactions in 3D and 2D WL conduction are the dominant conductivity mechanisms in the samples at different temperature ranges [Fig. 1]. Assuming 2D transport σ_0 is found to be between 88 to 15 $S\text{ cm}^{-1}$ for these samples (Table I), which is one order smaller than the estimated minimum metallic conductivity for sp^2 -bonded (3D) a -C.¹⁰ These films behave like disordered metals with high conductivity. From $\sigma_{2D\text{ min}}$ for a 2D a -C film, an estimation of the effective sample thickness can be made as less than 10 nm (Ref. 10). σ_{min} is not derived from E_a since it remains uncertain at low temperatures.^{3,4} Based on the diffusion coefficient D_i (maximum $\sim 1\text{ cm}^2/\text{s}$) and phase breaking time $\tau_\phi (> 10^{-10}\text{ s})$ [determined from MR at 4.2 K in the following section] $L_{Th} = (D_i \tau_\phi)^{1/2}$ was found to be larger than the effective thickness of the samples establishing 2D conduction (Table I). The characteristic length $L_c \sim (hD_i/2\pi kT)^{0.5}$ was also used to determine the dimensionality of the samples.¹⁰ From the fitted value of ‘ m ’ and D_i in Eq. (1) the upper limit of L_c has been calculated at 4.2 K (see Table I). Both L_c and L_{Th} for C_{600} are larger than for NCD_{20N} and NCD_{10N} films.⁸ These derived values are also slightly smaller than the diameter of WL orbits suggested earlier,³ however they are consistent with microstructure of the films see (Refs.

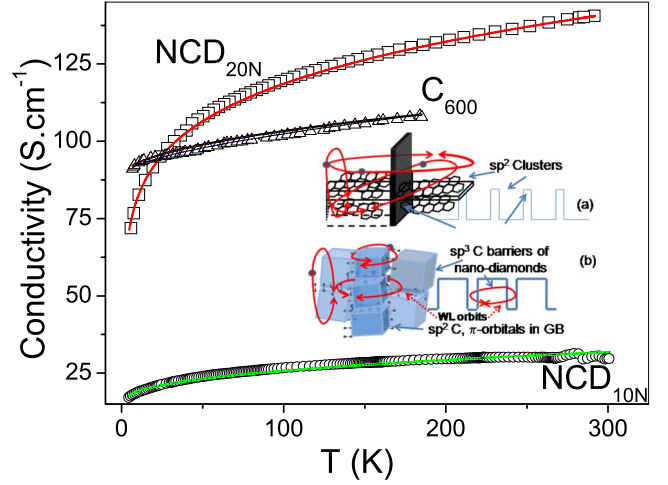


FIG. 2. (Color online) Model fit of conductivity for NCD_{20N} , NCD_{10N} , and C_{600} films. Inset: Proposed microstructure and electronic band structure of (a) C_{600} and (b) NCD_{20N} films showing WL localization orbits of different scale and some sp^2 -bonded structures for a -C films and π -orbitals within GB.

11–13) and the following discussion. The calculated values of D_i (see Table I) for these samples are slightly smaller than for graphitic carbon, but they are larger than for many other forms of carbon such as one-dimensional pyrolyzed polymers.^{14,15}

IV. MAGNETORESISTANCE

To confirm the WL and any interference of electron wave functions in the present systems, MR is studied from which the temperature dependence of τ_ϕ and elastic-scattering time (τ_0) can be determined.^{8,9,14} The conductivity of C_{600} shows WL at $T < 100\text{ K}$ [Fig. 1(b)], where a change of the sign of MR from positive (not shown here explicitly) to negative has been observed [Fig. 3(a)]. Using the previously proposed two band conduction model the positive MR [see Eq. (3)] and the typical value of electron mobility (μ) greater than $1\text{ cm}^2/\text{Vs}^{-1}$ at 100 K has been derived.^{8,9,14} This value is close to the reported value in nitrogen-doped NCD films and is obviously much greater than for 3D bulk a -C films ($10^{-6}\text{ cm}^2/\text{Vs}^{-1}$).^{2–4} Considering these models for sp^2 , a -C, and the values of elastic mean-free path (l_0) $\sim 1\text{ nm}$, the Fermi velocity (v_F) $\sim 10^6\text{ m/s}$, $m^* = 0.06m_0$, $\tau_0 = l_0/v_F = m^* \mu_0/e$, μ_0 (from positive MR, not shown here), and also using the relationship $D_i = v_F^2 \tau_0/2$, the values of τ_0 and D_i can be found to be around $6 \times 10^{-16}\text{ s}$ and $> 1\text{ cm}^2/\text{s}$, respectively.

TABLE I. Fitting parameters σ_0 , m , B , L_{Th} , and L_c of conductivity data shown in Fig. 2.

Sample	σ_0 ($S\text{ cm}^{-1}$)	m ($S/\text{cm K}^{1/2}$)	B (S/cm)	L_{Th} (m)	D_i (cm^2/s)	L_c (4 K)	Error (%)
NCD_{20N}	50	1.25	12.18	$\sim 1 \times 10^{-6}\text{ T}^{-3/2}$	0.4	101 Å	0.15
NCD_{10N}	15	0.70	0.81	$< 1 \times 10^{-6}\text{ T}^{-3/2}$	0.3	87 Å	0.25
C_{600}	88	1.45	0.18	$> 1 \times 10^{-6}\text{ T}^{-3/2}$	0.6	124 Å	0.42

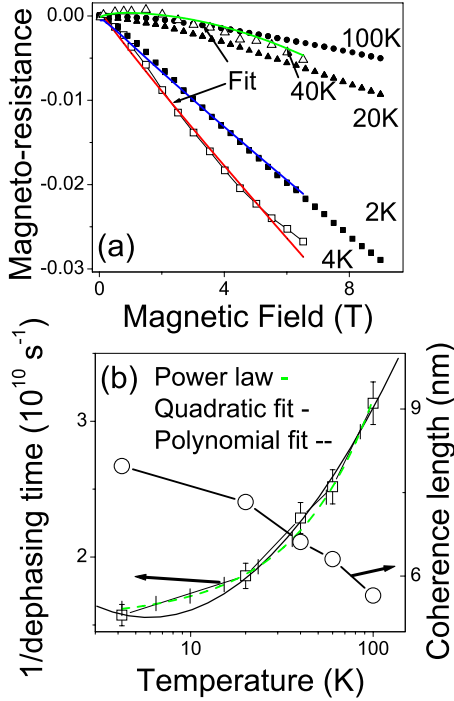


FIG. 3. (Color online) (a) Variation of magnetoresistance of NCD_{20N} (filled symbols) and C₆₀₀ films (open symbols) with magnetic field at different temperatures combined with a model fit using Eq. (3) for C₆₀₀ at 40 and 4 K and also for NCD_{20N} at 2 K. (b) Variation of L_φ and τ_φ^{-1} with T and different model fit of $\tau_\varphi^{-1}(T)$ for NCD_{20N}.

A remarkable similarity of MR for C₆₀₀ and NCD_{20N} samples as a function of H can be seen in Fig. 3(a) although the magnitude of negative MR of C₆₀₀ is lower than NCD_{20N} at a measured temperature. Therefore, all MR data for both samples are analyzed using a common approach and values of the derived parameters are found to be quite similar. We highlight the parameters for the NCD_{20N} sample and compare to C₆₀₀. We note that NCD samples in a previous report (cf. Ref. 3) showed a very similar kind of negative MR both in value and variation with H in the temperature range down to 2 K. To establish WL in these films we check the $H^{1/2}$ and $\ln H$ dependence of MR. We find a decrease in the slope of relative resistance $[\Delta\rho/\rho]$ versus $H^{1/2}$ curves with T [Fig. 3(a)] for both NCD_{20N} and C₆₀₀ samples, which to some extent is similar to other graphitic carbon whose magnetoconductance (MC) can be expressed as $\Delta\sigma(H, T) = \Delta\sigma_L^{2D}(H, T) + \Delta\sigma_I^{3D}(H, T)$ (Refs. 14 and 15). In the absence of the spin-orbit motion and magnetic impurities for 2D WL, MC is expressed as $\Delta\sigma_L^{2D}(H, T) = -e^2/\pi h [\Psi\{1/2 + H_\varphi/H\} - \ln\{H_\varphi/H\}]$, where Ψ and $H_\varphi(T)$ are the digamma function and the inelastic characteristic magnetic field, respectively.^{14,16} This expression can fit the data for 2D carbon only at low-field region.^{14,16} At low T and high H this equation can have an asymptotic behavior where $\Delta\sigma_L^{2D}(H, T) \sim \ln(H)$ and $\Delta\sigma_I^{3D}(H, T) = H^{1/2}$ (at $H/T \gg 1$) and $H^2/T^{1/2}$ (at $H/T \ll 1$), respectively,¹⁰ and MC can be expressed as

$$\Delta\sigma(H, T) = C_1 \ln(H) - C_2 H^{1/2} + C_3 T^{1/2}. \quad (2)$$

Equation (2) consists of $C_1 = e^2/\pi h \cdot \sigma(0, T) \sim 0.1$ T at 4 K, $C_2 = -[e^2 F/2\pi h][\pi g \mu_B H/2hD]^{0.5}$ and $C_3 = [1.3e^2 F/2\pi h][\pi k_B/2hD]^{0.5}$, with the electron screening parameter F and Boltzmann constant μ_B multiplied with the Lande ‘ g ’ factor (see Refs. 8–10). This equation can explain the negative MR along with 2D WL and also e–e interaction effects in the films but only in a qualitative manner. For the present experimental conditions, i.e., at 2 K and 9 T the asymptotic limit cannot be reached so that a proper fitting to MR data has not been obtained. It is important to note that here an external transverse magnetic field quenches the WL effect when it becomes greater than $H_\varphi(T) = h/\{8\pi e D_i \tau_\varphi(T)\}$. The logarithmic increase in the resistance due to WL will be suppressed except at a very low field where the 2D conductance can be written as $\Delta\sigma(0, T) \sim \ln(H_\varphi/H_0)$ (H_0 is the elastic characteristic magnetic field).^{14,16,17} Finally considering the entire range of T and H , MR $[\Delta R/R]$ for these samples can be expressed [by modifying Eq. (2)] as a first order approximation;

$$\frac{\Delta R}{R} = \left(\frac{\Delta R}{R}\right)_{\text{Lorentz}} + \left(\frac{\Delta R}{R}\right)_{\text{WL}} + \left(\frac{\Delta R}{R}\right)_{\text{Interaction}} = C_0(\mu H^2) + C_1 \ln(H) + C_2 H + C_3(H^{0.5}) + C_4(T^{0.5}). \quad (3)$$

From data fitting (except at high field) at 4 K the parameters $C_0 = 1 \times 10^{-6}$, $C_1 = 3.8 \times 10^{-4}$, $C_2 = -4 \times 10^{-3}$, $C_3 = -2.5 \times 10^{-3}$, and $C_4 = 1 \times 10^{-3}$ can be derived, which shows both 2D WL and e–e interactions have a major contribution to the negative MR. At high T (i.e., >40 K), $\Delta R/R$ can be expressed as $-0.00013H^2 + 0.0002 \ln H + \text{a constant}$ showing the effect of 2D WL and the Lorentz term. Since H_0 (~ 1 T) remains fairly constant with temperature at $H < H_0$, and τ_0 ($\sim 1/H_0$) is very small ($\sim 10^{-16}$ s), the temperature dependence of MR and $H_\varphi(T)$ (~ 0.005 T at 4 K) in Eq. (3) can be used to determine $L_\varphi(T)$ and $\tau_\varphi(T)$. The temperature dependence of τ_φ has been found to follow a (weak) power-law ($\tau_\varphi \sim T^{-1.16}$) dependence rather than an exponential growth or a polynomial fit with the coefficients 0.74 and 1.05 for the first and second orders, respectively [Fig. 3(b)]. Considering only the inelastic scattering within the limit of error, and using $L_\varphi = (h/8\pi e H_\varphi)^{0.5} = \sqrt{2(D_i^2 m^* W/\pi k T)^{1/3}}$ (W represents the width of the 2D channel) the minimum value of $\tau_\varphi = L_\varphi^2/D_i$ can be obtained as 10^{-10} to 10^{-12} s for $L_\varphi \sim 1$ –10 nm, respectively. Interestingly, both in NCD films and C₆₀₀, τ_φ and L_φ are weakly temperature dependent [Fig. 3(b)] and this trend differs from graphitic carbon.^{14–17} On the other hand, these parameters, particularly the value of the exponent of temperature in the power-law fit, was found to be very similar to that of multiwalled nanotubes¹⁸ establishing the effect of the disorder induced e–e interaction in low-dimensional systems.

V. MICROSTRUCTURE AND PROPOSED MODEL

Comparing with disordered conducting carbon (C₆₀₀), we propose a microscopic model of NCD films [Fig. 2(a) and 2(b)]. All these investigated films contain confined sp^2 -C

pathways of length ~ 10 nm, which is shorter than both L_C and L_{Th} . Therefore, a real electronically 2D a -C system at low temperature can be proposed. At higher temperatures, L_c becomes shorter than the effective sample thickness and the interaction effect particularly in 2D cannot be seen. For C_{600} , tunnel barriers of disordered sp^3 -bonded carbon between sp^2 -bonded planar clusters are very thin, which can explain 2D WL via coherent tunnel transport through these barriers.⁶ For NCD sp^2 -bonded carbon layers are separated by thick (energetically high) barriers of diamond [Fig. 2(b)]. Here electrons could be confined and their tunneling probability through diamond should be reasonably low. However, due to a long L_φ and WL orbit, wave functions can interfere across the diamond nanocrystals showing WL in 2D and also a signature of e-e interactions. At high T , since the localization length of electron wave function becomes smaller than L_φ , a cross over from diffusion to hopping conduction is noticed.⁴ This analysis is in agreement with the microscopic observation of the GB, which is about 2-nm thick^{1,11} and WL study in NCD films.³ The negative MR in the VRH regime can also be caused by the dephasing effects of H by the interference

between hopping paths whose length can be determined via $H_\varphi(T)$ (Ref. 19).

VI. CONCLUSIONS

Our results are consistent with previous reports on the analysis of the electrical transport of NCD films.¹⁻⁴ However in this report we added a new understanding of microstructure using tunneling and weakly localized transport, which should be verified with additional experiments. Here we showed a new set of values of m^* , L_φ , and τ_φ in the modified and confined structure of low-dimensional carbon that can be useful for developing high-speed devices over large area.²⁰

ACKNOWLEDGMENTS

The author is thankful to Andre Strydom, University of Johannesburg for his help in the experiment and the late A.R. Krauss and D.M. Gruen and other group members of Argonne National Laboratory for providing necessary support in the past, which was useful to complete this work.

*Author to whom correspondence should be addressed. somnath.bhattacharyya@wits.ac.za

¹S. Bhattacharyya, O. Auciello, J. Birrell, J. A. Carlisle, L. A. Curtiss, A. N. Goyette, D. M. Gruen, A. R. Krauss, J. Schlueter, A. Sumant, and P. Zapol, *Appl. Phys. Lett.* **79**, 1441 (2001); D. M. Gruen, *Annu. Rev. Mater. Sci.* **29**, 211 (1999).

²P. Achatz, O. A. Williams, P. Bruno, D. M. Gruen, J. A. Garrido, and M. Stutzmann, *Phys. Rev. B* **74**, 155429 (2006).

³J. J. Mares, P. Hubik, J. Kristofik, D. Kindl, M. Fanta, M. Nesladek, O. Williams, and D. M. Gruen, *Appl. Phys. Lett.* **88**, 092107 (2006).

⁴O. A. Williams, S. Curat, J. E. Gerbi, D. M. Gruen, and R. B. Jackman, *Appl. Phys. Lett.* **85**, 1680 (2004); S. Bhattacharyya, *Phys. Rev. B* **70**, 125412 (2004).

⁵T. Sarda and S. Bhattacharyya, in *Encyclopedia of Nanoscience and Nanotechnology*, edited by H. S. Nalwa (American Scientific, Valencia, CA, 2004), Vol. 2, pp. 337-370.

⁶S. Bhattacharyya, *Appl. Phys. Lett.* **91**, 142116 (2007).

⁷S. Bhattacharyya, S. J. Henley, E. Mendoza, L. G-Rojas, J. Al-lam and S. R. P. Silva, *Nat. Mater.* **5**, 19 (2006).

⁸L. Al'tshuler and A. G. Aronov, *Sov. Phys. JETP* **50**, 968 (1979).

⁹N. F. Mott and M. Kavesh *J. Phys. C* **14**, L659 (1984); A. Lee and T. V. Ramakrishnan, *Rev. Mod. Phys.* **57**, 287 (1985); N. F. Mott, *Metal-Insulator Transitions* (Taylor & Fransis, London, 1990).

¹⁰G. Du, V. N. Prigodin, A. Burns, J. Joo, C. S. Wang, and A. J.

Epstein, *Phys. Rev. B* **58**, 4485 (1998).

¹¹J. Birrell, J. E. Gerbi, O. Auciello, J. M. Gibson, D. M. Gruen, and J. A. Carlisle, *J. Appl. Phys.* **93**, 5606 (2003).

¹²P. Zapol, M. Sternberg, L. A. Curtiss, T. Frauenheim, and D. M. Gruen, *Phys. Rev. B* **65**, 045403 (2001).

¹³F. Cleri, P. Klebniski, L. Colombo, D. Wolf, and S. R. Phillpot, *Europhys. Lett.* **46**, 671 (1999).

¹⁴A. A. Bright, *Phys. Rev. B* **20**, 5142 (1979); V. Bayot, L. Piraux, J.-P. Michenaud, J.-P. Issi, M. Lelaurain, and A. Moore, *ibid.* **41**, 11770 (1990).

¹⁵K. Takai, M. Oga, H. Sato, T. Enoki, Y. Ohki, A. Taomoto, K. Suenaga, and S. Iijima, *Phys. Rev. B* **67**, 214202 (2003).

¹⁶V. Bayot, L. Piraux, J.-P. Michenaud, and J.-P. Issi, *Phys. Rev. B* **40**, 3514 (1989); L. Piraux, V. Bayot, J. P. Issi, M. S. Dresselhaus, M. Endo, and T. Nakajima, *ibid.* **41**, 4961 (1990); R. T. F. van Schaijk, A. de Visser, S. G. Ionov, V. A. Kulbachinskii, and V. G. Kytin, *ibid.* **57**, 8900 (1998).

¹⁷H. R. Shea, R. Martel, and Ph. Avouris, *Phys. Rev. Lett.* **84**, 4441 (2000).

¹⁸N. Kang, J. S. Hu, W. J. Kong, L. Lu, D. L. Zhang, Z. W. Pan, and S. S. Xie, *Phys. Rev. B* **66**, 241403(R) (2002).

¹⁹S. Roche, F. Triozon, A. Rubio, and D. Mayou, *Phys. Lett. A* **285**, 94 (2001).

²⁰K. S. Novoselov, A. K. Geim, S. V. Morozov, D. Jiang, M. I. Katsnelson, I. V. Grigorieva, S. V. Dubonos and A. A. Firsov, *Science* **306**, 666 (2004).